High resolution soil moisture monitoring using active heat pulse method with fiber optic temperature sensing at field scale

D.N. Vidana Gamage[1], A. Biswas [2] and I.B. Strachan[1]

[1]McGill University, Department of Natural Resource Sciences, Montreal, Canada.

[2]School of Environmental Sciences, University of Guelph, Guelph, Canada

A paper from the Proceedings of the
14th International Conference on Precision Agriculture
June 24 – June 27, 2018
Montreal, Quebec, Canada

Abstract. *Knowledge of spatial and temporal variability of soil moisture is critical for site specific irrigation management at field scale. However, installation feasibility, cost and between-sensor variability restrict the use of many point–based sensors at field scale. Active heat pulse method with fiber optic temperature sensing (AHFO) has shown a potential to provide soil moisture data at sub-meter intervals along a fiber optic cable to a distance >10000 meters. Despite the limited number of studies on soil moisture measurement using AHFO, this study evaluated the feasibility of AHFO to provide soil moisture data at sub meter (spatial) and diurnal to seasonal (temporal) scales in a subsurface drained field. Heat pulses of five minutes durations were applied at a rate of 7.28 Wm^{-1} through six fiber optic cable transects installed at three depths (0.05, 0.10 and 0.20 m) at six hours interval in a day. A distributed temperature sensing (DTS) instrument was used to estimate the cumulative temperature increase (T_{cum}) at locations along the cable. Indirect relationships between T_{cum} and soil moisture was developed and validated for each depth using the soil moisture measured by the commercial point–based sensors (calibrated by the gravimetric method). Sigmoidal (logistic) relationship provided the best fit between soil moisture and T_{cum} for the three depths with R^2 values of 0.89, 0.91 and 0.91 respectively. In comparison to the calibrated commercial soil moisture sensors, AHFO showed predictive accuracies; RMSE of 3, 4 and, 4 % for 0.05,0.10 and 0.2 m depths, respectively. Further, it showed strong agreement between AFHO predicted and commercial sensors measured soil moisture values; correlation coefficient (r) of 0.87, 0.46 and 0.86 for the three depths, respectively. Results of this study showed the capability of AHFO method to provide soil moisture data at sub-meter intervals (spatial) along the fiber optic cable transects and diurnal to seasonal scales (temporal) with satisfactory accuracy.*

Keywords. *soil moisture, active heat pulse method, spatial and temporal variation*

1. Introduction

There is the growing need for the development of efficient irrigation management practices due to increasing irrigation water scarcity as a result of growing population and changing climate. Monitoring spatial and temporal variation of soil moisture at field scale is a pre-requisite to develop efficient irrigation management practices. The efficiency of the irrigation management practices depends on the ability to monitor the spatial variability of soil moisture and its time evolution at field scale which helps to define and track the plant available moisture content in soils.

Monitoring soil moisture content (SMC) in the laboratory using the thermogravimetric method is labor-intensive (Gooley et al., 2014) while point–based sensors such as TDR and neutron probes can yield a decent spatial coverage if measured manually specially at plot to field scale. However, the manual SMC measurements are time-consuming with a relatively coarse temporal resolution (e.g., weekly, or monthly). By contrast, automated sensors such as capacitance and FDR probes with data logging capacity can record SMC data at high temporal resolution (e.g. minutes to hours) but their cost and between sensor variability restricts the installation at high densities over larger areas. This inherent disconnection in the spatial and temporal coverage in soil moisture measurement hinders accurate characterization of spatial and temporal dynamics of subsurface and/or vadose zone hydrology at field scale. Although there is a broad range of soil moisture sensors are available, their potential applications for high resolution soil moisture monitoring at field scale is limited. This calls for alternates to the current sensing techniques in improving the SMC measurement to better monitor and characterize the spatial and temporal dynamics of soil moisture at field scale.

Several methods have emerged to measure SWC at the field scale including Cosmic ray probes (Ragab et al., 2017; Zreda et al., 2008), electromagnetic induction sensors (EMI) (Abdu et al., 2008; Moghadas et al., 2017), GPS reflectometry (Larson et al., 2008) and AHFO (Ciocca et al., 2012; Gil-Rodríguez et al., 2013; Sayde et al., 2014; Sayde et al., 2010). Among these techniques, AHFO is attractive because of its potential to measure soil moisture at sub-meter intervals along a fiber optic cable up to 10,000 m lengths. Therefore, the AHFO technique has the potential to monitor soil moisture at high spatial and temporal resolutions and help to develop precision irrigation management practices at field scale. AHFO applies an electrically generated heat pulse to the fiber optic cable and the resulting temperature change (thermal response) during or after the heat pulse is related to the water content of the soil using either empirically or physically based equations. Despite the limited number of studies which have evaluated its feasibility to measure SMC at the laboratory scale (Ciocca et al., 2012; Gil-Rodríguez et al., 2013; Sayde et al., 2010), no studies have tested the feasibility of the AHFO technique using fiber optic cables buried in crop grown soils throughout a cropping season. Understanding the finer scale spatial structure of soil water in crop grown surface soils is important for precision irrigation scheduling (Hassan-Esfahani et al., 2017). The objective of this study was to test the feasibility of the AHFO technique to measure soil moisture in the surface soil of a crop grown field over a growing season using an *in-situ* calibration approach. Using an *in-situ* calibration approach can improve the efficacy of the measurement by integrating a modest network of the point–based sensors at the field scale and expected to minimize errors which can result due to use of repacked soil columns in the laboratory.

Overall, this study will examine, if the AHFO technique is a feasible tool for monitoring spatial and temporal soil moisture dynamics throughout a cropping season at the field scale.

2. Materials and methods

2.1 Site description

The study site was a 4.2 ha experimental corn field located near Saint Emmanuel, Coteau du Lac, Quebec, Canada (Figure 1a) approximately 60 km west of Montréal. The soil is classified as a Soulanges very fine sandy loam (Lajoie and Stobbe, 1951), has a mean depth of 0.50 - 0.90 m and overlies clay deposits from the Champlain Sea. The field has a flat topography, with an average slope of less than 0.5% (Kaluli et al., 1999). The study site consisted of three blocks (A, B and C) and each block comprised eight sub plots (15 m × 75 m). In the center of each sub plot, a tile drain had been installed at 1.0 m depth. These drains discharge into two buildings located on the northern side of the field (Figure 1a).

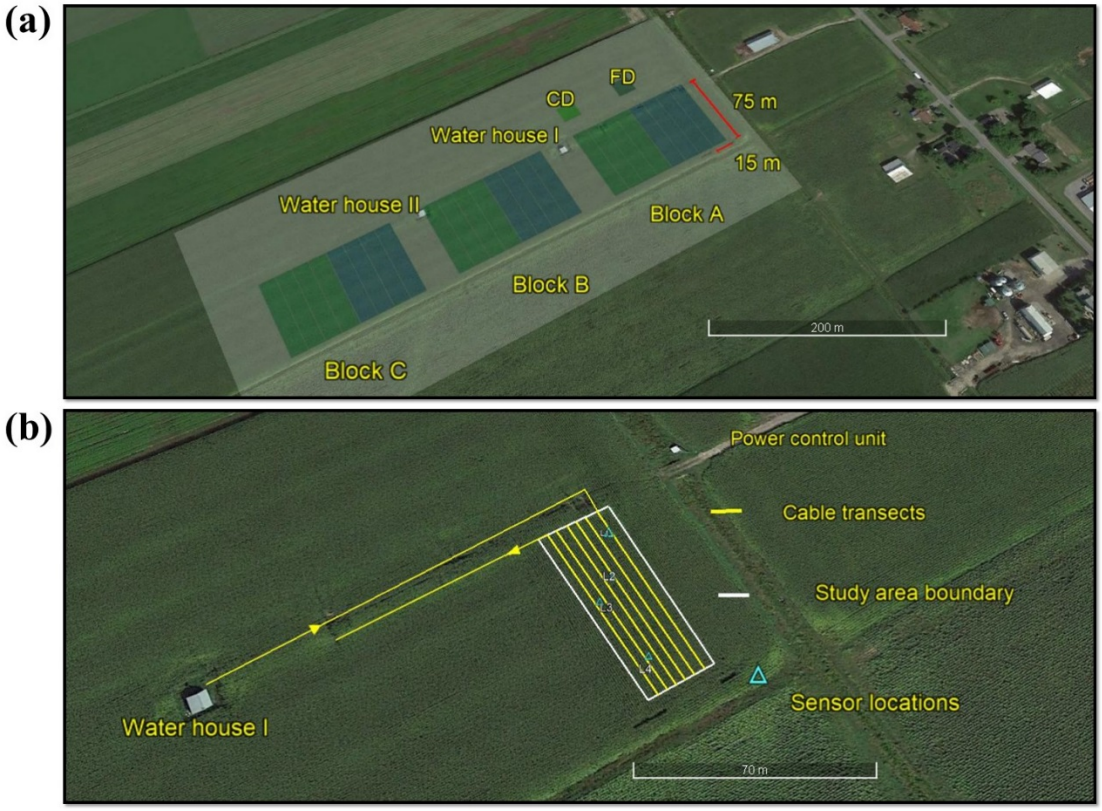

Fig. 1 (a) Shows the study area which consists of three main blocks A, B and C. Blue and green rectangles within the main block are sub plots (15×75 m) free drainage (FD) and controlled drainage(CD). Two water houses facilitate the measurement of drainage volume from each sub plot. (b) shows the fiber optic cable configuration in the field. Cable connected to the DTS instrument starts from the water house I and runs through two subplots at three depths (0.05, 0.10 and 0.20 m), blue rectangles show the locations of 5TE sensors used for calibration and validation.

2.2 Distributed temperature tensing system

The AHFO technique uses the DTS system which measures the environmental temperature at sub-meter spatial intervals along a fiber optic cable up to lengths of 10000 m. The DTS system consisted of a DTS instrument and a fiber optic cable connected to it. The DTS instrument used in this study was a Linear Pro series DTS (N4386B, AP Sensing, Germany) and it had two channels with a maximum measurement range of 4 km. The fiber optic cable (BRUsteel, Brugg Cable, Switzerland) consisted of a stainless steel loose tube containing four multimode 50 µm cores and 125 µm cladding fibers; the steel tube was armored with stainless steel strands and was further enclosed in a protective nylon jacket. The external cable diameter was 3.8 mm.

2.3 Fiber optic cable installation

A custom designed plow was used to install the fiber optic cable into 18 transects at three depths 0.05, 0.10 and 0.20 m (6×3) in two sub plots of Block A (Figure 1b) on 10 June 2016. Three separated fiber optic cable spools mounted on top the plow were simultaneously fed through three steel tubes attached at the back of the plow blade in six parallel passes of 73.6 ± 0.3 m long (including the turns). The distance between two successive cable transects was 3.75 m. A duplex single ended calibration set up (Hausner et al., 2011) was achieved by connecting the near cable end (to the DTS instrument) from 0.05 m depth to channel 1 of the DTS instrument, splicing the far cable ends from depths 0.05 and 0.10 m together and splicing the near cable ends from depth 0.10 and 0.20 m together.

2.4 Fiber optic cable heating

A domestic electrical grid supplied single-phase electricity to a step-up transformer (15J4Q5D1, Electric Power, Inc., Mississauga, Ontario, Canada) which converted the 120 V to 240 V. After the transformer, a main electrical box including a digital timer (ET1105C, Intermatic, Canada) was established. Three pairs of electrical cables (P1, P2, and P3) from the main electrical box were used for heating (Figure 2a). For a given depth, a fiber optic cable section of two consecutive transects was considered as a single heating section. Accordingly, P1, P2, and P3 were connected to heating section 1 (transects 1 and 2), 2 (transects 3 and 4) and 3 (transects 5 and 6), respectively. This allowed the development of fiber optic cable sections (147.3 m long) with similar heating characteristics. At each connecting location, approximately 0.10 m of the protective nylon jacket of the fiber optic cable was removed, and electrical cables were connected (Figure 2b). The electrical connections were enclosed in special plastic containers filled with insulating resin (ScotchcastTM 82-A1, Austin, Texas, USA) (Figure 2c) to avoid the risk of electrical shock. 240 volts were applied to each heating section to produce heat pulses of 7.28 W m^{-1} that were sent through all the fiber optic cable sections every six hours during a day starting from 12.00 am on the morning of 22 July 2016 to the 6.00 pm on the evening of 17 October 2017. A Heating duration of five minutes was used in this study based on the results of previous laboratory experiments which tested both high power (short) pulses and low power (long) pulses (Vidana Gamage and Biswas, 2016). A digital timer (synchronized with PC time) controlled the start and stop of the heat pulses while both voltage and current intensity were monitored. The DTS instrument (synchronized with PC time) recorded temperature continuously every 30 seconds along the fiber optic cable (0.25 m sampling interval) during the experimental period.

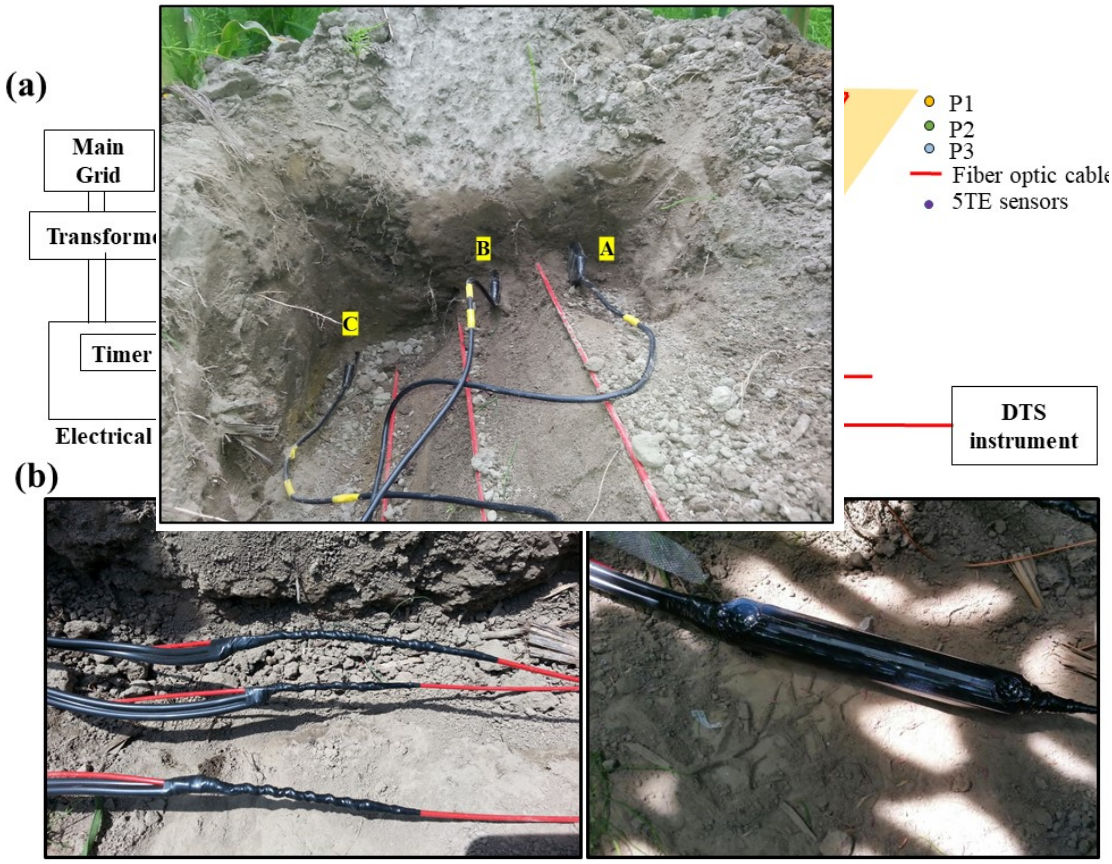

Fig. 2 (a) Schematic of the power supply from the electrical grid, transformer and main electrical board including the digital timer which controlled the heat pulses (on right), electrical cables pairs connected to each heating cable section (on left), (b) shows the electrical connections made to the metal sheath of the fiber optic cable (wrapped with electrical insulating tape), (c) an electrical connection enclosed in a plastic container filled with insulating resin.

2.5 Calibration and validation

Soil moisture data for calibration and validation were collected using nine 5TE soil moisture sensors (Decagon Devices, Pullman, WA, USA) calibrated using the gravimetric method installed at 0.05, 0.10 and 0.20 m depths in four reference cable transect locations. At each reference location, the soil was excavated (1 m long x 0.20 m width x 0.25 m depth) and soil moisture sensors were installed approximately 0.05 m away from the fiber optic cables (Figure 3). Ice bags were used to precisely locate 0.5 m long cable sections at each depth within a 1m long reference location (using the thermal signature; cables sections of low temperature). Soil moisture content at each reference locations was measured every five minutes by 5TE sensors. Only soil moisture contents measured at corresponding heat pulse times (i.e., 12 am, 6 am, 12 pm and 6 pm) were used for calibration and validation.

Fig. 3 Shows three 5TE soil water sensors installed approximately 0.05 m away from the fiber optic cable, A: 0.05m, B: 0.10 m and C: 0.20 m depths in a reference location.

2.6 D

The integral of the cumulative temperature increase (T_{cum}) during a heat pulse (Sayde et al., 2010) was calculated at each point of the fiber optic cable using

$$T_{cum} = \int_0^{t_0} \Delta T dt \quad (1)$$

and

$$T_{cum\_N} = \frac{T_{cum}}{q} \quad (2)$$

where T_{cum} is the integral of the cumulative temperature increase (˚C s) during the total time of integration to (s) at a given point of the cable, ΔT is the DTS recorded temperature change from the pre–pulse temperature (˚C). T_{cum} is a function of soil thermal properties such as the thermal conductivity; higher thermal conductivity (high SWC), will lead to a higher rate at which the heat is conducted away from the cable resulting in a low T_{cum} at a given point on the cable. In this study, the average temperature calculated over five minutes prior to each heat pulse was used as the pre–pulse temperature. This average was subtracted from the temperature during the pulse to obtain the temperature increase, ΔT. T_{cum} was then calculated as the sum of the values obtained by multiplying ΔT by the time interval (30 sec) between measurements.

Accordingly, T_{cum} was calculated during every heat pulse at each point of the cable transects. T_{cum} was normalized by power intensity (q) of 7.28 W m^{-1} as T_{cum_N} using Eq. 2. Depth specific calibration relationships were developed using T_{cum_N} and SWC data

obtained only from three reference locations at respective depths (due to a technical problem of soil water sensors at one location, SWC data was used only from three reference locations).

3. Results and discussion

3.1 Calibration and validation

A sigmoidal relationship provided the best fit between and T_{cum_N} for the depth specific and single calibration relationships (0.05 m: R^2 = 0.90; 0.10 m: R^2 = 0.91; 0.20 m: R^2 = 0.91 and single calibration: R^2 = 0.79) with RMSE of 0.08, 0.12, 0.18 and 0.02, respectively (Figure 4). The relationship linking the T_{cum_N} –VWC showed a similar shape for all the curves, particularly for the 0.10 and 0.20 m depths and single calibration exhibited relationships across a wider range of VWC (Figure 4c and 4d). The sensitivity of T_{cum_N} increased in dry soil at an increasing rate and the rate decreased after reaching a VWC between 30–35 % for all the depths (Figure 4). As the water content in the soil surrounding the fiber optic cable increased, heat conduction away from the cable increased because the water's greater thermal conductivity decreased T_{cum_N}. However, as the VWC increased further (>30 %), any increase in thermal conductivity was less rapid which results in T_{cum_N} being less sensitive to actual changes in VWC. Accordingly, the thermal response of the fiber optic cable to the resistive heating yielded similar primary shapes for all the calibration relationships (Figure 4).

Scattered data points in the single calibration relationship indicated the hetoreogenity of the T_{cum_N} under similar soil water contents at different depths (Figure 4a). This was particualy noticable for the 0.2 m depth; the magnitude of T_{cum_N} was hgiher compared to that of at 0.05 and 0.10 m depths under similar water conents (Figure 4b, c, and d). Possible reasons could be the presence of macro pores and/or air gaps at 0.20 m depth; most of the corn roots are distributed within 0.20–0.50 m depths as compared to shallow layers (Fan et al., 2016) which attributed to a relatively low bulk density. Further, soil pore size distribution and bulk densities can be different at reference locations from disturbance during installation. Transient nature of the soil structure healing could also lead to differences in pore size distribution around the cable. This could introdue a transient contact resisitance between the soil and the cable (Sourbeer and Loheide, 2016). Any decrase or increase in contact resistance might have lead to over and under estimation of VWC. Therefore, variations in pore size distribution and bulk densities could account for some of the scatter about the T_{cum_N}–VWC relationships (Figure 4). Despite the scattered data points, all the T_{cum_N}–VWC relationships were strong, particularly the depth specific T_{cum_N}– VWC relationships had the highest coeeficient of determinations (R^2) and used to predict the VWC along the fiber optic cable transects.

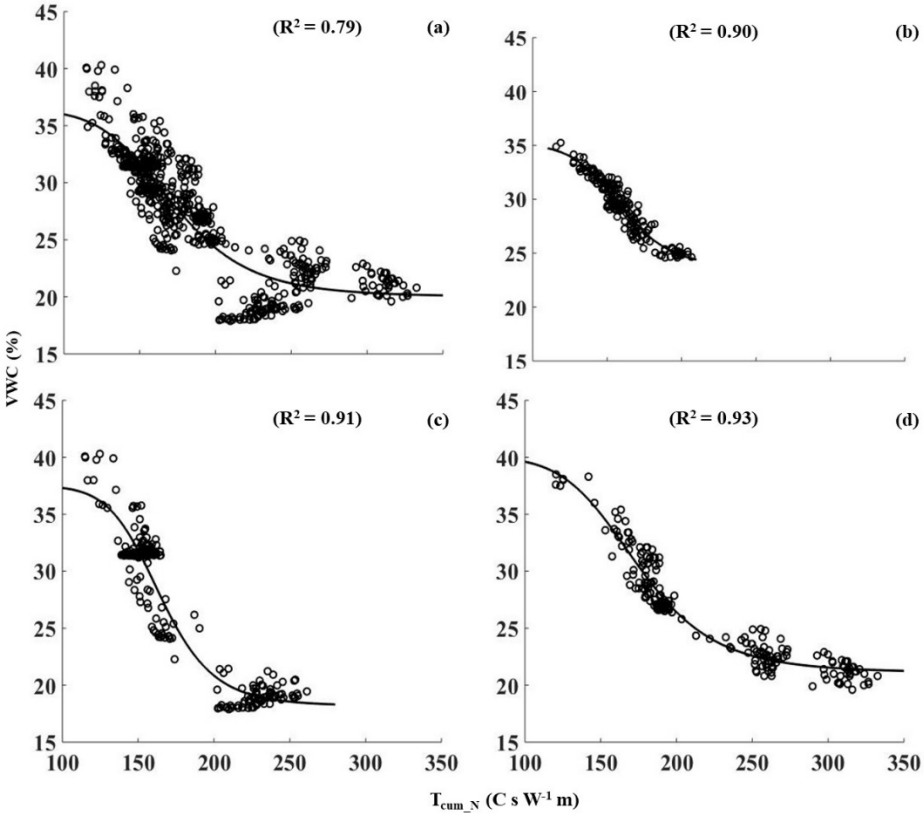

Fig. 4 Calibration relationships between soil moisture content (measured from the 5TE sensors installed near the reference cable locations in the field) and T_{cum_N} (thermal response measured by the DTS instrument at corresponding cable locations), (a) single calibration including all three depths, (b) depth 0.05 m, (c) 0.1 m and (d) 0.20 m depths, respectively.

The sensitivity of the calibration curve was dependent on the actual VWC measured by the 5TE sensors. Root mean square error of calibrated 5TE sensors was 2 % which suggested a good measurement accuracy. In comparison to the calibrated 5TE soil moisture sensors, AHFO showed predictive accuracies; RMSE of 3.3, 2.8, 3.7 and, 3.7 % for single calibration, 0.05, 0.10 and 0.2 m depths, respectively. Excellent agreements (R^2 = 0.87 and R^2 = 0.86) between observed and predicted VWC by the AHFO technique were observed except for 0.10 m depth (R^2 =0.46) (Figure 5). It should be noted that a technical problem at one sensor location resulted in a relatively small number of measurement points (N = 172) being used for validation of the 0.10 m depth. Lowest prediction error (RMSE = 2.8 %) and highest R^2 of 0.87 in validation statistics for 0.05 m depth indicated the ability of the AHFO technique to measure VWC in surface soils accurately. It also indicated an advantage of using the T_{cum} method which was corrected for pre-pulse or back ground temperature (Eq.1).

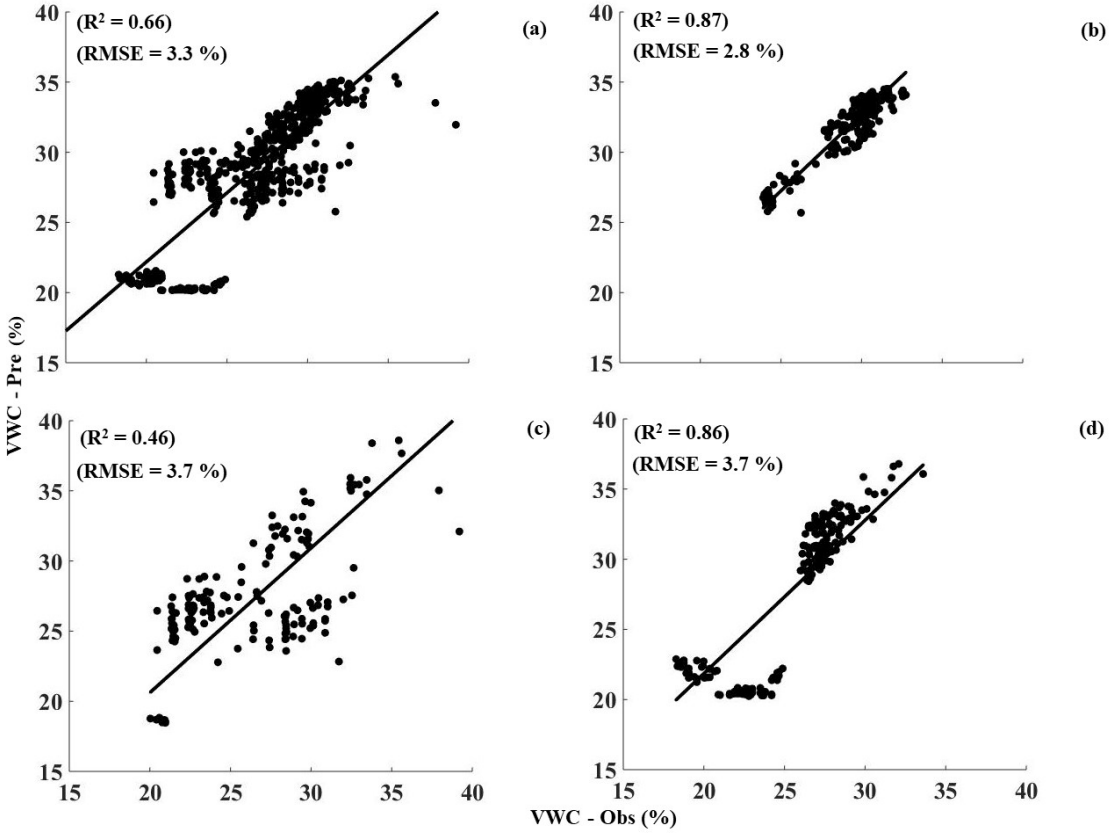

Fig. 5 Comparison between observed soil water content by 5TE sensors and predicted soil water content by AHFO technique (black dots) and black lines are the best fitted lines, (a) single calibration including all three depths, (b) 0.05 m, (c) 0.01 m and (d) 0.20 m depths, respectively.

3.2 Monitoring variability of soil water using AHFO technique

To examine the feasibility of the AHFO technique to detect the soil moisture changes at the field scale, we explored the ability of the AHFO technique to detect rainwater infiltration into the soil within a selected 24–hour period (12.00 am 13 August–12.00 am 14 August 2016; Figure 6). VWC predicted by the AHFO technique showed good agreement with rainfall events. VWC at 0.05 m depth showed that a rapid increase in response to rainfall occurred between 6 am and 12 pm (Figure 6c). Corresponding cable locations of the 0.10 m depth clearly showed a time lagged increase in VWC (Figure 6d). The deeper layer (0.20 m) was relatively wetter than the 0.10 m layer during the dry period (from 12 am to 6 am 13th August 2016), and this resulted in no visible time lagged increase in VWC at the deeper layer. Moreover, there was a rainfall event of <0.5 mm during the time from 12 am to 6 am (Figure 6a), however, it was not sufficient to increase the VWC in 0.10 and 0.20 m depths while a little increase in VWC was visible in 0.05 m depth (Figure 6c). These results suggested that the fiber optic cable could respond to

small variations in VWC of surface soil. Marked spatial variation in VWC along the transect was found in the shallow (0.05 m) layer compared to the deeper layers. Furthermore, the temporal patterns of VWC measured from the 5TE sensors and the mean VWC across the transect from the AHFO technique are nearly identical, despite their different measurement volumes (Figure 6b). This agreement showed that the AHFO technique could reliably track soil water changes and demonstrated the feasibility of using this technique at the field scale.

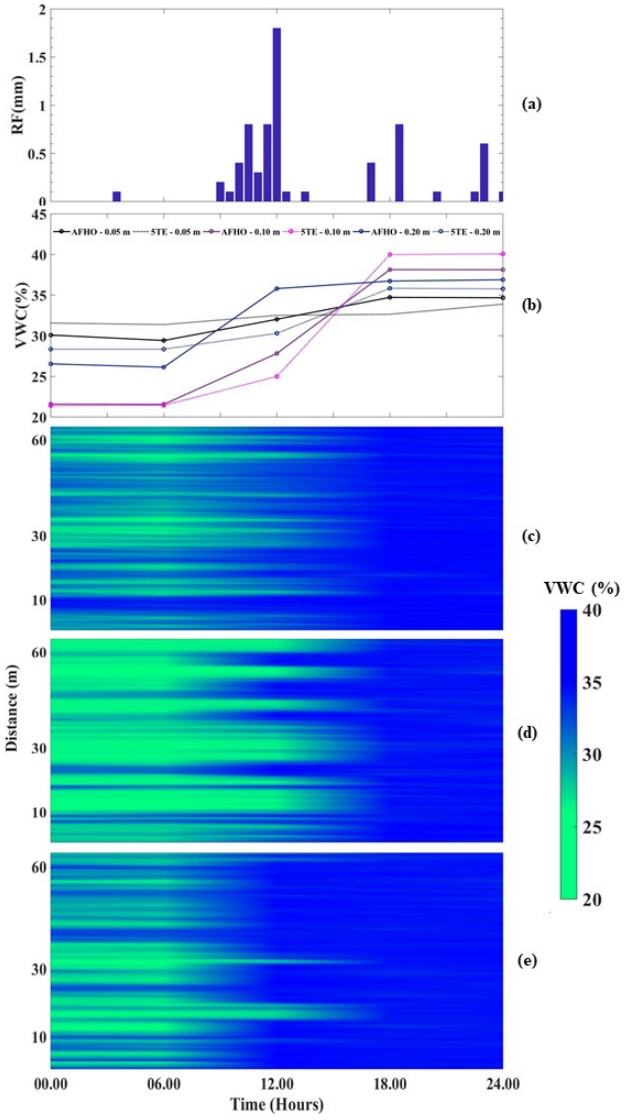

Fig.6 (a) Shows the pattern of rainfall during the period from 12 am 13th August 2016 to 12 am 14th August 2016 (24 hours period). (b) shows the changes in soil water content from the 5TE sensors at three depths in the transect 1 during the similar period, (c–e) shows the changes of mean soil water content of the transect 1 predicted by AHFO technique at 0.05, 0.10 and 0.20 m depths, respectively.

While quantification of spatial and temporal dynamics of soil water is beyond the scope of this paper, VWC predicted from the AHFO technique displayed a positive correlation with precipitation, as expected (Figure 7). The surface soil was drier during the period from July to mid-August 2016 which could be attributed to a lack of rainfall and high evaporation from the soil during the early growth of the corn. These findings were consistent with those of other studies (Liu et al., 2010; Zhang et al., 2011). VWC was comparatively higher and mostly related to the rainfall events that occurred during the period from mid-August to mid October 2016 (Figure 7). In addition, a soil water gradient from transect 1 to 6 was evident during the same period which demonstrated the variation in the distribution of surface soil water after rainfall events. However, more analysis is necessary to interpret the observed spatial and temporal variations of VWC.

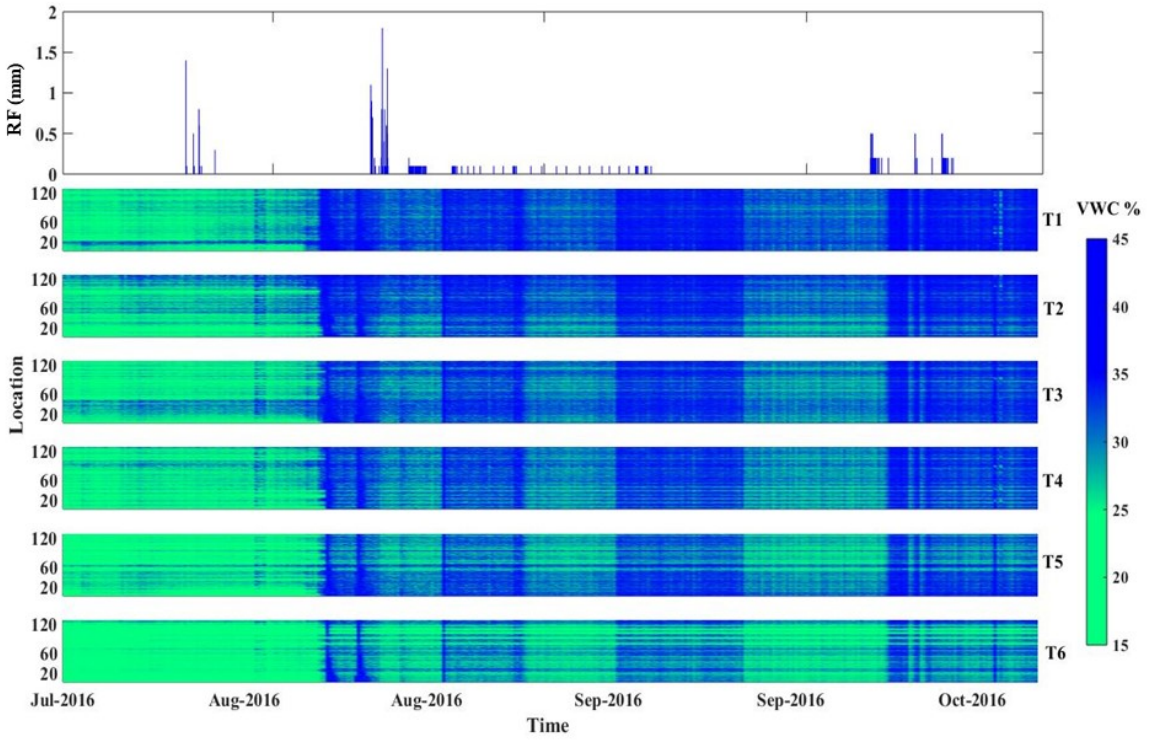

Fig.7 Variation of soil water content at every 0.5 m (location) along the six transects (T1 to T6) during the period from 22nd July 2016 to 17th October 2016 in response to rainfall at 0.05 m depth.

4. Conclusions

This study examined the feasibility of the AHFO technique to measure soil moisture in the surface soil of a crop grown field over a growing season. Depth specific strong calibration relationships between SWC and NT_{cum} predicted SWC with satisfactory accuracy when compared with calibrated commercial soil water sensors (RMSE = 2.8, 3.7 and 3.7% respectively). Further, strong agreements between AHFO predicted and 5TE sensors measured SWC were found at depths. The AHFO technique could accurately monitor the normal SWC variations of surface soil resulting from rainfall at diurnal to seasonal scales in a cropped field. Use of an *in-situ* calibration approach improved the efficacy of the

measurement by integrating a modest network of point–based sensors at the field scale. Overall, this study showed a great potential of the AHFO technique to measure soil water at high spatial resolutions (<1 m) and to monitor soil water dynamics of surface soil in a crop grown field over a cropping season with a reasonable compromise between accuracy and practicality. Future research is needed to determine the impact of thermal contact resistant on soil moisture measurement in heterogenous soils.

Acknowledgments

This project was funded by grants to Asim Biswas from FRQNT (Fonds de recherche du Québec-Nature et technologies, 2015-NC-180817) and NSERC (Natural Sciences and Engineering Research Council of Canada, RGPIN-2014-04100). The authors would also like to thank Helene Lalande for her assistance in the laboratory measurements and Guy Vincent, Maxime Leclerc and Yakun Zang, Kelly Nugent, Scott MacDonald, Tracy Rankin, Mi Lin and Rasika Burghate for assistance in cable installation and retrieval in the field.

References

Abdu, H., Robinson, D. A., Seyfried, M., and Jones, S. B. (2008). Geophysical imaging of watershed subsurface patterns and prediction of soil texture and water holding capacity. *Water Resources Research* **44**, W00D18.

Ciocca, F., Lunati, I., Van de Giesen, N., and Parlange, M. B. (2012). Heated Optical Fiber for Distributed Soil-Moisture Measurements: A Lysimeter Experiment. *Vadose Zone J* **11**, -.

Fan, J., McConkey, B., Wang, H., and Janzen, H. (2016). Root distribution by depth for temperate agricultural crops. *Field Crops Research* **189**, 68-74.

Gil-Rodríguez, M., Rodríguez-Sinobas, L., Benítez-Buelga, J., and Sánchez-Calvo, R. (2013). Application of active heat pulse method with fiber optic temperature sensing for estimation of wetting bulbs and water distribution in drip emitters. *Agricultural Water Management* **120**, 72-78.

Gooley, L., Huang, J., Pagé, D., and Triantafilis, J. (2014). Digital soil mapping of available water content using proximal and remotely sensed data. *Soil Use and Management* **30**, 139-151.

Hassan-Esfahani, L., Torres-Rua, A., Jensen, A., and McKee, M. (2017). Spatial Root Zone Soil Water Content Estimation in Agricultural Lands Using Bayesian-Based Artificial Neural Networks and High- Resolution Visual, NIR, and Thermal Imagery. *Irrigation and Drainage* **66**, 273-288.

Hausner, M. B., Suarez, F., Glander, K. E., van de Giesen, N., Selker, J. S., and Tyler, S. W. (2011). Calibrating Single-Ended Fiber-Optic Raman Spectra Distributed Temperature Sensing Data. *Sensors* **11**, 10859-10879.

Kaluli, J. W., Madramootoo, C. A., Zhou, X., MacKenzie, A. F., and Smith, D. L. (1999). Subirrigation Systems to Minimize Nitrate Leaching. *Journal of Irrigation and Drainage Engineering* **125**, 52-58.

Lajoie, P. G., and Stobbe, P. C. (1951). "Soils Study of Soulanges and Vaudreuil Counties in the Province of Quebec," Edmond Cloutier, Ottawa.

Larson, K. M., Small, E. E., Gutmann, E. D., Bilich, A. L., Braun, J. J., and Zavorotny, V. U. (2008). Use of GPS receivers as a soil moisture network for water cycle studies. *Geophysical Research Letters* **35**, L24405.

Liu, Y., Li, S., Chen, F., Yang, S., and Chen, X. (2010). Soil water dynamics and water use efficiency in spring maize (Zea mays L.) fields subjected to different water management

practices on the Loess Plateau, China. *Agricultural Water Management* **97**, 769-775.

Moghadas, D., Jadoon, K. Z., and McCabe, M. F. (2017). Spatiotemporal monitoring of soil water content profiles in an irrigated field using probabilistic inversion of time-lapse EMI data. *Advances in Water Resources* **110**, 238-248.

Ragab, R., Evans, J. G., Battilani, A., and Solimando, D. (2017). The Cosmic-ray Soil Moisture Observation System (Cosmos) for Estimating the Crop Water Requirement: New Approach. *Irrigation and Drainage* **66**, 456-468.

Sayde, C., Benitez Buelga, J., Rodriguez-Sinobas, L., El Khoury, L., English, M., van de Giesen, N., and Selker, J. S. (2014). Mapping variability of soil water content and flux across 1-1000 m scales using the Actively Heated Fiber Optic method. *Water Resources Research* **50**, 7302-7317.

Sayde, C., Gregory, C., Gil-Rodriguez, M., Tufillaro, N., Tyler, S., van de Giesen, N., English, M., Cuenca, R., and Selker, J. S. (2010). Feasibility of soil moisture monitoring with heated fiber optics. *Water Resources Research* **46**, W06201.

Sourbeer, J. J., and Loheide, S. P. (2016). Obstacles to long-term soil moisture monitoring with heated distributed temperature sensing. *Hydrological Processes* **30**, 1017-1035.

Vidana Gamage, D. N., and Biswas, A. (2016). Comparison of Power and Heating Time in Fiber Optic Distributed Temperature Sensing to Measure Soil Water. *In* "2016 CSSS/PRSSS Annual Meeting", pp. 83, Thompson Rivers University, Kamloops, BC.

Zhang, S., Li, P., Yang, X., Wang, Z., and Chen, X. (2011). Effects of tillage and plastic mulch on soil water, growth and yield of spring-sown maize. *Soil and Tillage Research* **112**, 92-97.

Zreda, M., Desilets, D., Ferré, T. P. A., and Scott, R. L. (2008). Measuring soil moisture content non-invasively at intermediate spatial scale using cosmic-ray neutrons. *Geophysical Research Letters* **35**, L21402.